This document is the accepted manuscript version of the following article:
Aksoyoglu, S., & Prévôt, A. S. H. (2018). Modelling nitrogen deposition: dry deposition velocities on various land-use types in Switzerland. International Journal of Environment and Pollution, 64(1-3), 230-245. https://doi.org/10.1504/IJEP.2018.10020573

Modelling nitrogen deposition: dry deposition velocities on various land-use types in Switzerland

S. Aksoyoglu and A.S.H. Prévôt

Laboratory of Atmospheric Chemistry (LAC), Paul Scherrer Institute (PSI), Forschungsstrasse 111, 5232 Villigen PSI, Switzerland

Email: sebnem.aksoyoglu@psi.ch

Email: andre.prevot@psi.ch

Abstract

In this study, we analyzed nitrogen deposition in Switzerland obtained from a modelling study in Europe for 2006 with the CAMx model. Comparison of modelled ammonia with measurements showed a relatively good agreement for annual concentrations whereas an overestimation was found in spring due to the meteorological conditions prevailing in 2006. The modelled average annual nitrogen deposition of 12.2 kg N ha^{-1} a^{-1} in Switzerland was dominated by the deposition of reduced nitrogen compounds (74%) and the largest contribution to nitrogen deposition was from dry deposition of ammonia. Dry deposition velocities of oxidized and reduced nitrogen compounds were calculated for specific land-use types found in Switzerland. The highest annual deposition velocities for ammonia and nitric acid were estimated over evergreen shrubs whereas the deposition was lowest over water surfaces. Deposition velocities over various land surfaces were shown to vary seasonally and the values in spring and summer were higher than in winter by a factor of up to 2.7.

Keywords: nitrogen; ammonia; dry deposition velocity; reduced nitrogen; oxidised nitrogen; land-use; evergreen shrubs; seasonal variation; CAMx; Switzerland.

1 Introduction

Nitrogen (N) is an essential nutrient for plant growth but excess N deposition has adverse effects such as acidification, eutrophication, and toxicity to plants (Jones et al., 2014). Excess N deposition might also lead to the loss of plant diversity (Roth et al., 2013; 2015). The oxidized and reduced nitrogen species are emitted from various sources. Nitrogen oxide, NO is emitted into the atmosphere by both natural sources like lightning and soil and by human activities related to combustion processes and then it is converted to other oxides of nitrogen (e.g. NO_2, HNO_3, N_2O_5, NO_3, PAN, organic nitrates). The reduced N compounds (primarily ammonia, NH_3), on the other hand, derive mainly from agricultural activities and form particulate ammonium (NH_4^+) after reacting with acids in the atmosphere.

Nitrogen compounds are removed from the atmosphere by dry and wet deposition processes leading to negative impacts on various ecosystems. In order to understand these impacts, it is necessary to quantify the deposition of nitrogen compounds. Assessment of nitrogen deposition is mostly achieved by chemical transport models (CTM) due to the complexity of measurements, especially for dry deposition fluxes. The current regional CTMs use similar deposition models such as wet scavenging of pollutants by precipitation and dry deposition based on resistance approach (Wesely, 1989, Zhang et al., 2003). There might be however, significant differences between the results of models using similar deposition schemes. For example, Vivanco et al. (2017) reported that there were large differences in dry deposition estimates of six regional CTMs used in the EURODELTA III exercise in Europe and pointed out the importance of correct estimation of dry deposition.

Modelling studies indicate that the dry deposition of reduced N (NH_3, NH_4^+) is the most important contributor to N deposition in central Europe (Dentener et al., 2006). The decline in N deposition between 1990 and 2005 in Europe was shown to be mainly related to the oxidized fraction due to

large reductions in NO_x ($NO+NO_2$) emissions in the past; the deposition of reduced N, however, was predicted to increase further until 2020 (Aksoyoglu et al., 2014; Simpson et al., 2014).

Dry deposition velocities that are required to calculate the deposition flux are derived from models that account for the reactivity, solubility and diffusivity of gases, local meteorological conditions, and season-dependent surface characteristics. In this study, in addition to the contribution of wet and dry deposition of nitrogen compounds to the total N deposition calculated by the CAMx model, we also report the annual as well as seasonal dry deposition velocity of oxidized and reduced nitrogen compounds on land-use types found in Switzerland.

2 Method

2.1 Air quality modelling

We used the model data generated during a modelling study about the European air quality in 2006 in which the regional air quality model CAMx (comprehensive air quality model with extensions), version 5.40 (http://www.camx.com) was used in a domain covered Europe with a horizontal resolution of 0.250^o x 0.125^o (Aksoyoglu et al., 2014). There was a nested domain covering Switzerland with a higher resolution (0.083^o x 0.042^o). The meteorological parameters were calculated by the Weather Research and Forecasting Model (WRF-ARW), version 3.2.1 (http://wrf-model.org/index.php). The initial and boundary conditions for the WRF model were provided by the ECMWF data (http://www.ecmwf.int/). We used 31 terrain-following σ-layers up to 100 hPa in WRF and then we selected 14 of them for CAMx, with the first layer being 20 m thick. The gas-phase mechanism was CB05 (Yarwood et al., 2005) and SOAP aerosol model was selected with fine/coarse option for the particle size. The initial and boundary concentrations were obtained from the MOZART (Model of Ozone and Related Chemical Tracers) global model for the studied period (Horowitz et al., 2003). The photolysis rates were calculated by the TUV model (http://cprm.acd.ucar.edu/Models/TUV/) and the ozone column densities were extracted from the TOMS data (http://ozoneaq.gsfc.nasa.gov/OMIOzone.md). We used the TNO/MACC emission inventory for the anthropogenic emissions in Europe (Denier van der Gon et al., 2010). We replaced the values in grid cells within the Swiss national boundary with the high-resolution Swiss emission data (INFRAS, 2010; Heldstab and Wuethrich, 2006; Kropf, 2001; Heldstab et al., 2003; Kupper et al., 2010). We calculated the emissions of biogenic volatile organic compounds (BVOC) such as isoprene, monoterpenes and sesquiterpenes with our own model using the temperature and shortwave irradiance from the WRF output (Andreani-Aksoyoglu and Keller, 1995; Oderbolz et al., 2013). More details about the model parameterization can be found in Aksoyoglu et al. (2014).

2.2 Deposition

Wet deposition: The wet deposition is the dominant removal process for particles. In CAMx, it is calculated using a scavenging approach in which the local rate of concentration change within or below a precipitating cloud depends on a scavenging coefficient. The wet deposition refers to the uptake of material into cloud/fog water and precipitation, and its subsequent transfer to the surface. CAMx uses 3-dimensional gridded distribution of cloud and precipitation water contents (liquid, snow and ice “graupel”) calculated by the meteorological model WRF. The two processes calculated for gases are direct diffusive uptake of ambient gases into falling precipitation and growth of cloud droplets that contain dissolved gases. For particles, the calculated components are impaction of ambient particles into falling precipitation and growth of cloud droplets that contain particle mass. The external inputs required by the CAMx wet deposition algorithm include the three-dimensional gridded distribution of cloud and precipitation water contents, with the precipitation contents broken down into liquid, snow and ice (ENVIRON, 2011). Rain, snow and graupel particles are represented separately. The efficiency of deposition processes to remove pollutants from the air depends on the physical and chemical properties of the pollutants, local meteorological conditions, the surface on which they are being deposited and on the frequency, duration, and intensity of precipitation events.

Dry deposition: Dry deposition is usually treated as a first-order removal mechanism where the flux of a pollutant to the surface is the product of a characteristic deposition velocity and its concentration in the surface layer. For a given species, particle size and grid cell, CAMx determines a deposition velocity for each land-use type in that cell and then linearly combines them according to the fractional distribution of land-use classes. Between the two options offered in CAMx, we selected the updated resistance model of Zhang et al. (2003) to calculate the dry deposition of gases. The 3-resistance equation for calculating deposition velocity includes aerodynamic, boundary and canopy resistances (ENVIRON, 2011). CAMx uses diffusion, impaction and/or gravitational settling for surface deposition of particles.

Although bi-directional air-surface exchange (dry deposition and emission) of NH_3 has been observed over a variety of land surfaces, the majority of the air quality models treat this exchange only as dry deposition which might lead to underestimation of daytime NH_3 concentration due to overestimation of dry deposition (Zhang et al., 2010). Winchink Kruit et al. (2012) reported that the inclusion of a stomatal compensation point increased modeled ammonia concentrations especially in agricultural source areas in the Netherlands. Ammonia stomatal compensation points are affected by the canopy type, temperature, growth stage, meteorological conditions, nitrogen status and cutting practices. It is therefore very difficult to implement it in chemical transport models (CTMs) mostly due to the missing knowledge of sub-grid variations in concentration, vegetation type and fertilizer applications (Huijsmans et al., 2018; Skjoth et al., 2011). Although introduction of compensation point improves the model performance, modeling of ammonia remains challenging due to temporal and spatial variations of emissions and grid resolution (Sutton et al., 2013). CAMx does not address bi-directional ammonia flux. It does however, use a deposition parameter that strongly influences ammonia deposition by changing the surface resistance.

3 Results and Discussion

3.1 Concentrations of ammonia and ammonium

A general model performance evaluation for the simulations used in this study was discussed elsewhere (Aksoyoglu et al., 2014). In this paper, we focus only on the model results relevant for nitrogen deposition. Ammonia is a key pollutant that plays an important role in the formation of atmospheric aerosols. Agriculture contributes about 93-95% to the total ammonia emissions in Switzerland (Kupper et al., 2015). Atmospheric ammonia concentrations have been monitored at various sites in Switzerland since 2000 (Thoeni and Seitler, 2013). The modelled annual ammonia concentrations are shown in Fig. 1 together with the measurement sites available in 2006. The model predicted elevated ammonia concentrations (3 - 12 $\mu g\ m^{-3}$) mainly over the Swiss Plateau. Comparison of modelled annual mean NH_3 concentrations with measurements using passive samplers at several sites suggests that CAMx could reproduce the annual ammonia concentrations reasonably well (Fig. 2). One should note that the measurements at several sites (e.g. 5 sites in Eschenbach, 8 sites in Wauwil) which are very close to each other and therefore belong to the same model grid cell, were averaged. The variability in such measurements is between 13-32% depending on the different agricultural activities. The highest concentrations measured at sites with intensive cattle farming in central Switzerland were captured quite well while concentrations were underestimated at stations mainly in southern Switzerland. On the other hand, there was some overestimation at a few elevated sites.

Analysis of long-term (10 years) measurement data indicated that the seasonal variation of ammonia emissions might vary depending on the meteorological conditions prevailing each year. An example at two measurement stations Taenikon and Payerne is shown in Fig. 3. Temperature and wind speed are generally the most important drivers for ammonia emissions (Huijsmans et al., 2018). In general, the highest emissions are in spring and there are usually increased levels in summer and fall. This typical seasonal variation is caused by evaporation of ammonia with warmer temperatures and by the agricultural activities (manure application in spring, manure storage activities in late fall). Country wise ammonia emission distributions for specific

agricultural emission categories suggest that there are differences in agricultural practice that lead to significant differences between countries (Skjoth et al., 2011). On the other hand, Thoeni and Seitler (2013) showed that the lowest ammonia emissions in Switzerland occur in winter (December, January), highest in spring (March, April), and there are often some peaks in summer and late fall. In 2006, however, the maximum ammonia concentrations were measured in summer and they were relatively low in spring (Fig. 3) most likely due to the shifted manure applications as a consequence of an unusually cold and long winter. This led to a discrepancy between the modelled and measured ammonia in spring (Fig. 4, left panel) since temporal profiles used in the emission inventory for agricultural emissions are based on the common seasonal variations observed in Europe (Fig. 4, right panel). We compared the model results also with the available measurements of total ammonia and total nitrate at Payerne. Overestimated ammonia emissions in spring, lead to an over prediction of total ammonia (NH_3 + particulate NH_4^+) while measurements and model results agree reasonably well in other seasons as shown in Fig. 5 (left). The modelled total nitrate (HNO_3 + particulate NO_3^-) on the other hand, was underestimated in winter (Fig. 5, right panel). In addition to the difficulties in reproducing the meteorological parameters in winter (Aksoyoglu et al., 2014) and uncertainties in NO_x emissions (Oikonomakis et al., 2018), modelling ammonium nitrate concentrations is especially challenging because it resides in both the gas and the aerosol phase. The equilibrium between the particulate ammonium nitrate and its gaseous precursors HNO_3 and NH_3 strongly depends on temperature and relative humidity. Moreover, dry deposition of HNO_3 is very fast. Therefore, when the equilibrium in the model shifts more towards the gas-phase, rapid removal of nitric acid might lead to an underestimation of total nitrate.

3.2 Nitrogen deposition

The model output for deposition consists of dry and wet deposition of each species. The total nitrogen deposition was calculated by summing dry and wet deposited amounts of both oxidized and reduced nitrogen compounds. The average total nitrogen deposition in Swiss grid cells was predicted to be 12.2 kg N ha^{-1} a^{-1} with the largest values found in central Switzerland where NH_3 emissions are the highest (Fig. 6, left panel). Deposition of reduced N compounds (blue colours in Fig. 6, right panel) was about 74% of the total nitrogen deposition with dry NH_3 deposition being the dominant fraction. The spatial distributions of dry deposition of NH_3 and HNO_3 and wet deposition of NH_4^+ and NO_3^- are shown in Fig. 7. Dry deposition of NH_3 varies between 5 and 20 kg N ha^{-1} a^{-1} over the Swiss Plateau with higher values up to almost 40 kg N ha^{-1} a^{-1} in a small area around Lucerne with intensive cattle farming. On the other hand, deposition of oxidized N compounds is much lower than those of reduced N species. These results are in the same range as those obtained by inferential deposition methods in 2010 by Rihm and Achermann (2016). Evaluation of modelled deposition is very challenging due to lack of measurements, especially of dry deposition. On the other hand, model performance for wet deposition is strongly limited by the quality of the meteorological data. The occult (fog) deposition might contribute significantly to deposition over forest canopies in the mountainous regions. Although it is a complex process, several studies showed that the WRF model was able to correctly simulate the liquid water content (LWC) and fog events in many cases (Roman-Cascon et al., 2016; Shimadera et al., 2011). We compared the modelled wet oxidized and reduced N deposition with a few measurements available at 13 sites in various parts of Switzerland (Fig. 8). The wet N deposition was underestimated by -30% and -55%, for reduced (left) and oxidized (right) N compounds, respectively, especially in the south of the Alps. These results seem to be reasonable considering the fact that differences between modelled and measured wet deposition of more than a factor of two are not uncommon especially at sites with complex topography (Schaap et al., 2004; Simpson et al., 2011; Solazzo et al., 2012; Vivanco et al., 2017).

3.3 Land use specific dry deposition velocities

We analyzed the effective dry deposition velocity for oxidized and reduced nitrogen compounds for the land-use types found in the Swiss grid cells. The annual dry deposition velocity of gaseous ammonia (NH_3) was determined to be the highest in the Swiss domain, followed by HNO_3 (Fig. 9).

On the other hand, deposition velocities of NO_2 and particulate species (NH_4^+ and NO_3^-) were much lower. Among the 26 land-use categories used in model simulations, deposition velocities of species were determined for 9 land-use types relevant for Switzerland. The fractional distributions of these land-use types in the grid cells as well as the annual average deposition velocities of HNO_3 and NH_3 over them are shown in Fig. 10. Mixed and evergreen needleleaf forests are the most abundant land-use types while others are more local, i.e. tundra in the Alpine regions, crops mainly in the Swiss Plateau. The highest annual deposition velocities were over evergreen shrubs (4.6 and 3.4 cm s^{-1}, for NH_3 and HNO_3, respectively) as well as deciduous broadleaf and evergreen needleleaf forests whereas the lowest values were predicted over water surfaces (0.9 and 0.8 cm s^{-1} for NH_3 and HNO_3, respectively).

In a review paper by Schrader and Brümmer (2014), the following ranges were reported for NH_3 deposition velocities in cm s^{-1}: for water 0.5-0.9, coniferous forests 0.5-3.3, deciduous forests 0.3-1.8, mixed forests 0.4-3.0, urban 0.1-1.1, agricultural land 0.2-7.1. These numbers however, are based on various measurements and models carried out at different times of the day, seasons and regions, making a comparison with our results difficult. For example, using the inferential method for ammonia over a Spruce forest in Germany, Zimmermann et al. (2006) derived a dry deposition velocity of 6 cm s^{-1} in the fall while the annual mean was 3.3 cm s^{-1}. On the other hand, in another model study over coniferous forests in Germany, an annual mean of 1.6 cm s^{-1} was reported (Builtjes et al., 2011). The deposition velocity of ammonia derived from the inferential method during hot season at two sites with mostly coniferous trees in Nova Scotia, Canada was shown to be much lower (0.5 cm s^{-1}) (Zhang et al., 2009). Some other studies reported ammonia deposition velocity of between 0.16 and 0.99 cm s^{-1} over central African tropical forests (Adon et al., 2013) and 1.3 cm s^{-1} over Alpine tundra in Colorado (Rattray and Sievering, 2001). Inferential modelling with four dry deposition routines applied across the NitroEurope network showed discrepancies in deposition velocities for NH_3 by up to a factor of 3 between models (Flechard et al., 2011). All these studies indicate that the dry deposition velocities might vary significantly depending on the method used, season and the region.

We also investigated the seasonal variation of dry deposition velocity of ammonia and nitric acid. As shown in Fig. 11, deposition velocities vary seasonally with the highest values in spring and summer over land surfaces. The largest difference between the lowest values in winter and highest ones in spring and summer was about a factor of 2.7 for both ammonia and nitric acid. Over the forests (coniferous, deciduous, mixed) there was no significant difference between spring and summer while over evergreen shrubs, the highest deposition velocities of ammonia and nitric acid were in summer (7.1 and 5.4 cm s^{-1}, respectively). Evergreen shrubs are found mostly at elevated sites around the Alpine regions (see Fig. 10) and they might still be covered by snow in spring, leading to lower dry deposition velocity compared to summer.

4 Conclusions

In this follow-up study of an earlier project about the modelling of the European air quality using the CAMx regional chemical transport model, we focused on nitrogen deposition in Switzerland in 2006. We first analysed the temporal and spatial variation of modelled ammonia concentrations. The temporal variation of ammonia in the emission inventory used in the model is based on the common practice in agricultural activities leading to highest emissions in spring and increased emissions again in summer and fall. Long-term measurements in Switzerland show that the seasonal variation of ammonia emissions might be different depending on the meteorological conditions prevailing each year. Comparisons with measurements performed at several sites showed a relatively good agreement for annual concentrations. On the other hand, an overestimation was found in spring due to the meteorological conditions prevailing in 2006 leading to relatively lower emissions in spring. These results showed the importance of using realistic seasonal variation of ammonia emissions in models since agricultural activities might be different following the meteorological conditions prevailing each year.

The modelled average annual nitrogen deposition of 12.2 kg N ha^{-1} a^{-1} in Switzerland was dominated by the deposition of reduced nitrogen compounds (74%) and the largest contribution

to nitrogen deposition was from dry deposition of ammonia. Dry deposition velocities of oxidized and reduced nitrogen compounds were calculated for specific land-use types found in Switzerland. The highest annual deposition velocities for ammonia and nitric acid were estimated over evergreen shrubs whereas the deposition was slowest over water surfaces. Deposition velocities over various land-use types were shown to vary seasonally and the highest values were calculated for spring and summer. The land-use-specific deposition velocities obtained in this study will provide valuable input for inferential models to calculate the deposition flux as well as for quick estimates of nitrogen deposition on ecosystems.

Acknowledgements

This study was financially supported by the Swiss Federal Office for the Environment, FOEN. We gratefully acknowledge Forschungsstelle fuer Umweltbeobachtung, FUB for providing us with the NH_3 measurement data and Beat Rihm for sharing the deposition data. We would also like to thank the following institutions for providing us with the weather, emission and measurement data: ECMWF, TNO, IIASA, INFRAS, Meteotest and NABEL/EMPA. We appreciate the continuous support of CAMx model developers at RAMBOLL.

References

Adon, M., Galy-Lacaux, C., Delon, C., Yoboue, V., Solmon, F., and Kaptue Tchuente, A. T. (2013) 'Dry deposition of nitrogen compounds (NO_2, HNO_3, NH_3), sulfur dioxide and ozone in west and central African ecosystems using the inferential method', *Atmos. Chem. Phys.,* 13, 11351-11374, 10.5194/acp-13-11351-2013.

Andreani-Aksoyoglu, S., and Keller, J. (1995) 'Estimates of monoterpene and isoprene emissions from the forests in Switzerland', *Journal of Atmospheric Chemistry*, Vol. 20, pp. 71-87.

Aksoyoglu, S., Keller, J., Ciarelli, G., Prévôt, A. S. H., and Baltensperger, U. (2014) 'A model study on changes of European and Swiss particulate matter, ozone and nitrogen deposition between 1990 and 2020 due to the revised Gothenburg protocol', *Atmospheric Chemistry and Physics*, Vol. 14, pp.13081-13095, 10.5194/acp-14-13081-2014.

Builtjes, P., Banzhaf, S., Gauger, T., Hendriks, E., Kerschbaumer, A., Koenen, M., Nagel, H.-D., Schaap, M., Scheuschner, & T., Schlutow, A. (2011) '*Erfassung, Prognose und Bewertung von Stoffeinträgen und ihren Wirkungen in Deutschland (in German language)'.* Report of the German Federal Environmental Agency (UBA), FKZ 3707 64 200.

Denier van der Gon, H., Visschedijk, A., van de Brugh, H., and Droege, R. (2010) *A high resolution European emission data base for the year 2005. A contribution to UBA-Projekt: "Strategien zur Verminderung der Feinstaubbelastung" – PAREST: Partikelreduktionsstrategien –Particle Reduction Strategies*, TNO, Utrecht (NL)TNO-034-UT-2010-01895_RPT-ML.

Dentener, F., Drevet, J., Lamarque, J. F., Bey, I., Eickhout, B., Fiore, A. M., Hauglustaine, D., Horowitz, L. W., Krol, M., Kulshrestha, U. C., Lawrence, M., Galy-Lacaux, C., Rast, S., Shindell, D., Stevenson, D., Van Noije, T., Atherton, C., Bell, N., Bergman, D., Butler, T., Cofala, J., Collins, B., Doherty, R., Ellingsen, K., Galloway, J., Gauss, M., Montanaro, V., Müller, J. F., Pitari, G., Rodriguez, J., Sanderson, M., Solmon, F., Strahan, S., Schultz, M., Sudo, K., Szopa, S., and Wild, O. (2006) 'Nitrogen and sulfur deposition on regional and global scales: A multimodel evaluation', *Global Biogeochemical Cycles*, 20, n/a-n/a, 10.1029/2005GB002672.

ENVIRON (2011), *CAMx User's Guide*, Comprehensive Air Quality Model with Extensions, Version 5.40, ENVIRON International Corporation, Novato, California, (www.camx.com)

Flechard, C. R., Nemitz, E., Smith, R. I., Fowler, D., Vermeulen, A. T., Bleeker, A., Erisman, J. W., Simpson, D., Zhang, L., Tang, Y. S., and Sutton, M. A. (2011), 'Dry deposition of reactive nitrogen to European ecosystems: a comparison of inferential models across the NitroEurope network', *Atmos. Chem. Phys*., 11 2703-2728, 10.5194/acp-11-2703-2011.

Heldstab, J. and Wuethrich, P. (2006) '*Emissionsmuster. Raeumliche Verteilung und Ganglinien fuer CO-/NMVOC-Emissionen'*, BAFU, Bern/Zurich, BAFU/INFRAS, 15.

Heldstab, J., de Haan van der Weg, P., Kuenzle, T., Keller, M., and Zbinden, R. (2003) *'Modelling of PM10 and PM2:5 ambient concentrations in Switzerland 2000 and 2010'*, Bundesamt fuer Umwelt, Wald und Landschaft (BUWAL), Bern, Environmental Documentation No. 169.

Horowitz, L. W., Walters, S., Mauzerall, D. L., Emmons, L. K., Rasch, P. J., Granier, C., Tie, X., Lamarque, J.-F., Schultz, M. G., Tyndall, G. S., Orlando, J. J., and Brasseur, G. P. (2003) 'A global simulation of tropospheric ozone and related tracers: Description and evaluation of MOZART, version 2.' , *Journal of Geophysical Research,* Vol. 108, pp. 4784, doi:10.1029/2002JD002853.

Huijsmans, J. F. M., Vermeulen, G. D., Hol, J. M. G., and Goedhart, P. W. (2018) 'A model for estimating seasonal trends of ammonia emission from cattle manure applied to grassland in the Netherlands', *Atmospheric Environment*, Vol. 173, pp. 231-238, https://doi.org/10.1016/j.atmosenv.2017.10.050.

INFRAS (2010) '*HBEFA, Handbuch Emissionsfaktoren des Strassenverkehrs'*, Version 3.1, INFRAS, UBA Berlin, UBAWien, BAFU, Bern.

Jones, L., Provins, A., Holland, M., Mills, G., Hayes, F., Emmett, B., Hall, J., Sheppard, L., Smith, R., Sutton, M., Hicks, K., Ashmore, M., Haines-Young, R., and Harper-Simmonds, L., (2014) 'A review and application of the evidence for nitrogen impacts on ecosystem services', *Ecosystem Services*, Vol. 7, pp. 76-88, http://dx.doi.org/10.1016/j.ecoser.2013.09.001.

Kropf, R. (2001) *Massnahmen zur Reduktion der PM10* – Emissionen, Umwelt – Materialien Nr. 136, Bundesamt fuer Umwelt (BAFU), 112, Bern.

Kupper, T., Bonjour, C., Achermann, B., Zaucker, F., Rihm, B., Nyfeler-Brunner, A., Leuenberger, C., and Menzi, H. (2010) '*Ammoniakemissionen in der Schweiz: Neuberechnung 1990–2007 Prognose bis 2020'*, Bundesamt fuer Umwelt (BAFU), Bern.

Kupper, T., Bonjour, C., and Menzi, H. (2015) 'Evolution of farm and manure management and their influence on ammonia emissions from agriculture in Switzerland between 1990 and 2010', *Atmospheric Environment*, 103, 215-221, http://dx.doi.org/10.1016/j.atmosenv.2014. 12.024.

Oderbolz, D. C., Aksoyoglu, S., Keller, J., Barmpadimos, I., Steinbrecher, R., Skjøth, C. A., Plaß-Dülmer, C., and Prévôt, A. S. H. (2013) 'A comprehensive emission inventory of biogenic volatile organic compounds in Europe: improved seasonality and land-cover', *Atmospheric Chemistry and Physics*, Vol. 13, pp. 1689-1712, 10.5194/acp-13-1689-2013.

Oikonomakis, E., Aksoyoglu, S., Ciarelli, G., Baltensperger, U., and Prévôt, A. S. H. (2018) 'Low modeled ozone production suggests underestimation of precursor emissions (especially NO_x) in Europe', *Atmospheric Chemistry and Physics,* 18, 2175-2198, 10.5194/acp-18-2175-2018.

Rattray, G., and Sievering, H. (2001) 'Dry deposition of ammonia, nitric acid, ammonium, and nitrate to alpine tundra at Niwot Ridge, Colorado', *Atmospheric Environment,* 35, 1105-1109, https://doi.org/10.1016/S1352-2310(00)00276-4.

Rihm B. and Achermann B. (2016) '*Critical Loads of Nitrogen and their Exceedances. Swiss contribution to the effects-oriented work under the Convention on Long-range Transboundary Air Pollution (UNECE)*', Federal Office for the Environment, Bern. Environmental studies no. 1642: 78 p.

Román-Cascón, C., Steeneveld, G. J., Yagüe, C., Sastre, M., Arrillaga, J. A., and Maqueda, G. (2016) 'Forecasting radiation fog at climatologically contrasting sites: evaluation of statistical methods and WRF', *Quarterly Journal of the Royal Meteorological Society,* 142, 1048-1063, doi:10.1002/qj.2708.

Roth, T., Kohli, L., Rihm, B., and Achermann, B. (2013) 'Nitrogen deposition is negatively related to species richness and species composition of vascular plants and bryophytes in Swiss mountain grassland', *Agriculture, Ecosystems & Environment*, 178, 121-126, http://dx.doi.org/10.1016/j.agee.2013.07.002.

Roth, T., Kohli, L., Rihm, B., Amrhein, V., and Achermann, B. (2015) 'Nitrogen deposition and multi-

dimensional plant diversity at the landscape scale', *Royal Society Open Science*, Vol. 2, 10.1098/rsos.150017.

Schaap, M., van Loon, M., ten Brink, H. M., Dentener, F. J., and Builtjes, P. J. H. (2004) 'Secondary inorganic aerosol simulations for Europe with special attention to nitrate', *Atmos. Chem. Phys.,* 4, 857-874, 10.5194/acp-4-857-2004.

Schrader, F. and Brümmer, C., (2014) 'Land use specific ammonia deposition velocities: a review of recent studies (2004-2013)', *Water, Air & Soil Pollution,* 225:2114

Shimadera, H., Kondo, A., Shrestha, K. L., Kaga, A., and Inoue, Y. (2011) Annual sulfur deposition through fog, wet and dry deposition in the Kinki Region of Japan, *Atmospheric Environment,* 45, 6299-6308, https://doi.org/10.1016/j.atmosenv.2011.08.055.

Simpson D., Wenche Aas, Jerzy Bartnicki, Haldis Berge, Albert Bleeker, Kees Cuvelier, Frank Dentener, Tony Dore, Jan Willem Erisman, Hilde Fagerli, Chris Flechard, Ole Hertel, Hans van Jaarsveld, Mike Jenkin, Martijn Schaap, Valiyaveetil Shamsudheen Semeena, Philippe Thunis, Robert Vautard and Massimo Vieno (2011) *Atmospheric transport and deposition of rective nitrogen in Europe,* In *"The European Nitrogen Assessment*", ed. Mark A. Sutton, Clare M. Howard, Jan Willem Erisman, Gilles Billen, Albert Bleeker, Peringe Grennfelt, Hans van Grinsven and Bruna Grizzetti. Published by Cambridge University Press.

Simpson, D., Andersson, C., Christensen, J. H., Engardt, M., Geels, C., Nyiri, A., Posch, M., Soares, J., Sofiev, M., Wind, P., and Langner, J. (2014) 'Impacts of climate and emission changes on nitrogen deposition in Europe: a multi-model study', *Atmospheric Chemistry and Physics*, 14, 6995-7017, 10.5194/acp-14-6995-2014.

Skjøth, C. A., Geels, C., Berge, H., Gyldenkærne, S., Fagerli, H., Ellermann, T., Frohn, L. M., Christensen, J., Hansen, K. M., Hansen, K., and Hertel, O. (2011) 'Spatial and temporal variations in ammonia emissions – a freely accessible model code for Europe', *Atmospheric Chemistry and Physics*, 11, 5221-5236, 10.5194/acp-11-5221-2011.

Solazzo, E., Bianconi, R., Pirovano, G., Matthias, V., Vautard, R., Moran, M. D., Wyat Appel, K., Bessagnet, B., Brandt, J., Christensen, J. H., Chemel, C., Coll, I., Ferreira, J., Forkel, R., Francis, X. V., Grell, G., Grossi, P., Hansen, A. B., Miranda, A. I., Nopmongcol, U., Prank, M., Sartelet, K. N., Schaap, M., Silver, J. D., Sokhi, R. S., Vira, J., Werhahn, J., Wolke, R., Yarwood, G., Zhang, J., Rao, S. T., and Galmarini, S. (2012) 'Operational model evaluation for particulate matter in Europe and North America in the context of AQMEII', *Atmospheric Environment*, 53, 75-92, http://dx.doi.org/10.1016/j.atmosenv.2012.02.045.

Sutton, M. A., Reis, S., Riddick, S. N., Dragosits, U., Nemitz, E., Theobald, M. R., Tang, Y. S., Braban, C. F., Vieno, M., Dore, A. J., Mitchell, R. F., Wanless, S., Daunt, F., Fowler, D., Blackall, T. D., Milford, C., Flechard, C. R., Loubet, B., Massad, R., Cellier, P., Personne, E., Coheur, P. F., Clarisse, L., Van Damme, M., Ngadi, Y., Clerbaux, C., Skjøth, C. A., Geels, C., Hertel, O., Wichink Kruit, R. J., Pinder, R. W., Bash, J. O., Walker, J. T., Simpson, D., Horváth, L., Misselbrook, T. H., Bleeker, A., Dentener, F., and de Vries, W. (2013) 'Towards a climate-dependent paradigm of ammonia emission and deposition', *Philosophical Transactions of the Royal Society B: Biological Sciences,* 368, 10.1098/rstb.2013.0166.

Thoeni, L., and Seitler, E. (2013) *Ammoniak-Immissionsmessungen in der Schweiz 2000 bis 2012*, Forschungsstelle fuer Umweltbeobachtung, FUB Report, Rapperswil.

Vivanco, M. G., Bessagnet, B., Cuvelier, C., Theobald, M. R., Tsyro, S., Pirovano, G., Aulinger, A., Bieser, J., Calori, G., Ciarelli, G., Manders, A., Mircea, M., Aksoyoglu, S., Briganti, G., Cappelletti, A., Colette, A., Couvidat, F., D'Isidoro, M., Kranenburg, R., Meleux, F., Menut, L., Pay, M. T., Rouïl, L., Silibello, C., Thunis, P., and Ung, A. (2017) 'Joint analysis of deposition fluxes and atmospheric concentrations of inorganic nitrogen and sulphur compounds predicted by six chemistry transport models in the frame of the EURODELTAIII project', *Atmospheric Environment*, 151, 152-175, http://dx.doi.org/10.1016/j.atmosenv.2016.11.042.

Wesely, M. L. (1989) 'Parameterization of surface resistances to gaseous dry deposition in regional-scale numerical models', *Atmospheric Environment*, 23, 1293-1304.

Wichink Kruit, R. J., Schaap, M., Sauter, F. J., van Zanten, M. C., and van Pul, W. A. J. (2012) 'Modeling the distribution of ammonia across Europe including bi-directional surface–atmosphere exchange', *Biogeosciences*, 9, 5261-5277, 10.5194/bg-9-5261-2012.

Yarwood, G., Rao, S., Yocke, M., and Whitten, G. Z. (2005) *Updates to the Carbon Bond chemical mechanism: CB05* Yocke & Company, Novato, CA 94945RT-04-00675.

Zhang L., Vet R., O'Brien J. M., Mihele C., Liang Z., and Wiebe, A.(2009) 'Dry deposition of individual nitrogen species at eight Canadian rural sites', *Journal of Geophysical Research: Atmospheres,* 114, doi:10.1029/2008JD010640.

Zhang, L., Brook, J. R., and Vet, R. (2003) 'A revised parameterization for gaseous dry deposition in air-quality models', *Atmospheric Chemistry and Physics*, 3 2067-2082, 10.5194/acp-3-2067-2003.

Zhang, L., Wright, L. P., and Asman, W. A. H. (2010) Bi-directional air-surface exchange of atmospheric ammonia: A review of measurements and a development of a big-leaf model for applications in regional-scale air-quality models, *Journal of Geophysical Research: Atmospheres,* 115, doi:10.1029/2009JD013589.

Zimmermann, F., Plessow, K., Queck, R., Bernhofer, C., and Matschullat, J.(2006) 'Atmospheric N- and S-fluxes to a spruce forest—Comparison of inferential modelling and the throughfall method', *Atmospheric Environment*, 40, 4782-4796, https://doi.org/10.1016/j.atmosenv.2006.03.056.

Figure Captions

Figure 1: Modelled annual mean NH_3 concentrations in 2006. Measurement sites are shown on the map.

Figure 2: Measured (from FUB) versus modeled (CAMx) annual mean NH_3 concentrations at various measurement sites in 2006. Measured values at several sites within the same model grid cell were averaged. The solid line is 1:1, dashed lines are 2:1 and 1:2 correlations.

Figure 3: Monthly variation of measured ammonia concentrations at Taenikon (blue) and Payerne (red) between 2002 and 2012 (data provided by FUB).

Figure 4: Monthly variation of modeled (blue) and measured (red) NH_3 concentrations at Payerne in 2006 (left) and the time profile of emission factors for NH_3 from agriculture given by the European TNO- MACC emission inventory (right).

Figure 5: Seasonal variation of measured (red) and modeled (blue) total ammonia (left) and total nitrate (right) at Payerne (2006).

Figure 6: Modeled N deposition in 2006 (kg N ha^{-1} y^{-1}) in Switzerland (left) and relative contribution of oxidized (red, orange, yellow) and reduced (blue tones) components to dry (65%) and wet (35%) deposition (right).

Figure 7: Modeled dry deposition of NH_3 (left upper panel), wet deposition of particulate NH_4^+ (right upper panel), dry deposition of HNO_3 (left lower panel) and wet deposition of particulate NO_3^- (right lower panel) in 2006 (kg N ha^{-1} y^{-1}).

Figure 8: Measured versus modeled wet NH_4^+ (left) and NO_3^- (right) deposition at 13 sites in Switzerland in 2006. Measurements were provided by the Swiss Federal Office of Environment (FOEN)

Figure 9: Spatial distribution of annual average dry deposition velocities (cm s^{-1}), upper panels: NH_3 (left), HNO_3 (right), lower panels: NO_2 (left) and NH_4^+ (right).

Figure 10: Fractional distribution of land-use types in grid cells of the Swiss domain and annual average dry deposition velocities (cm s^{-1}) of NH_3 and HNO_3 on these land-use types shown in Table.

Figure 11: Seasonal variation of dry deposition velocity (cm s^{-1}) for NH_3 (left) and HNO_3 (right) in 2006.

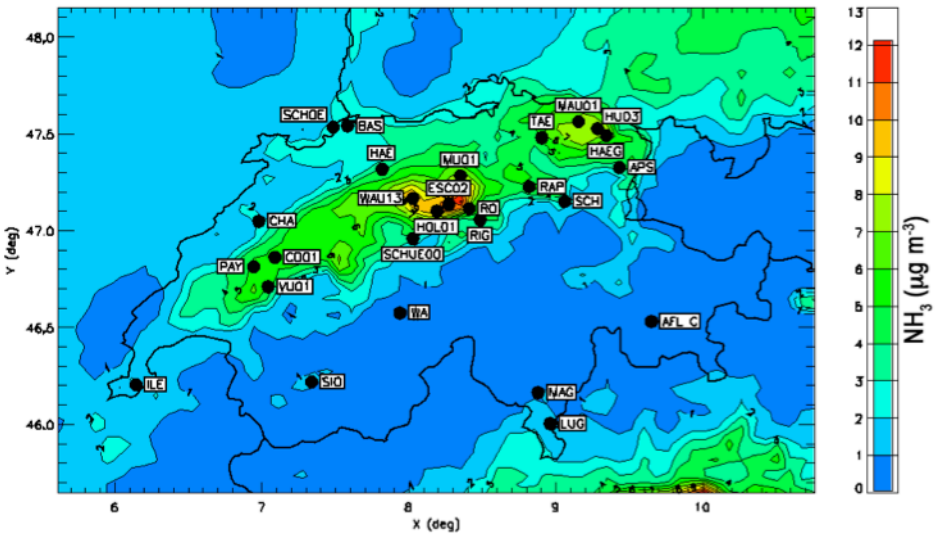

Figure 1: Modelled annual mean NH_3 concentrations in 2006. Measurement sites are shown on the map.

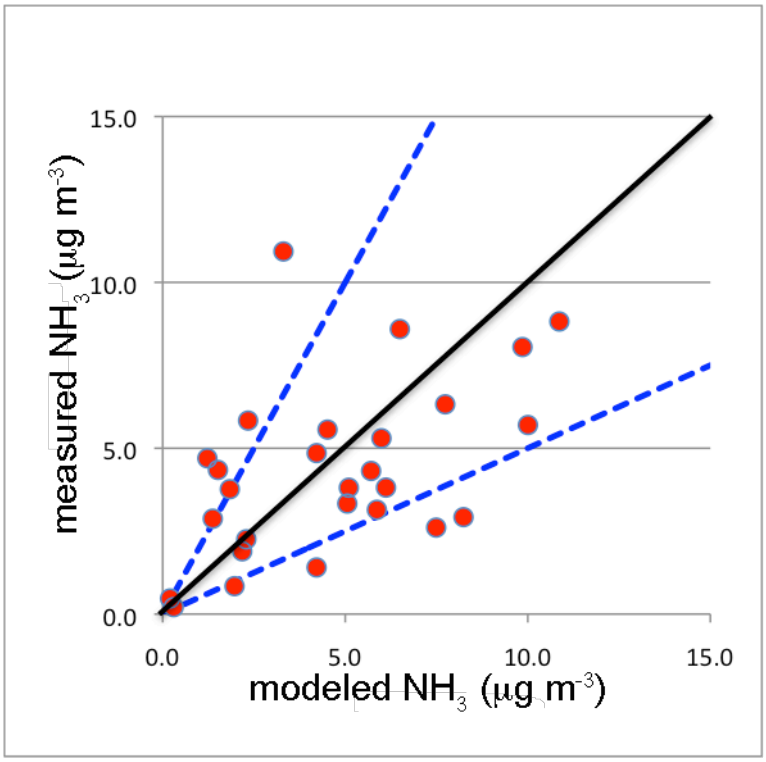

Figure 2: Measured (from FUB) versus modeled annual mean NH_3 concentrations at various measurement sites in 2006. Measured values at several sites within the same model grid cell were averaged. The solid line is 1:1, dashed lines are 2:1 and 1:2 correlations.

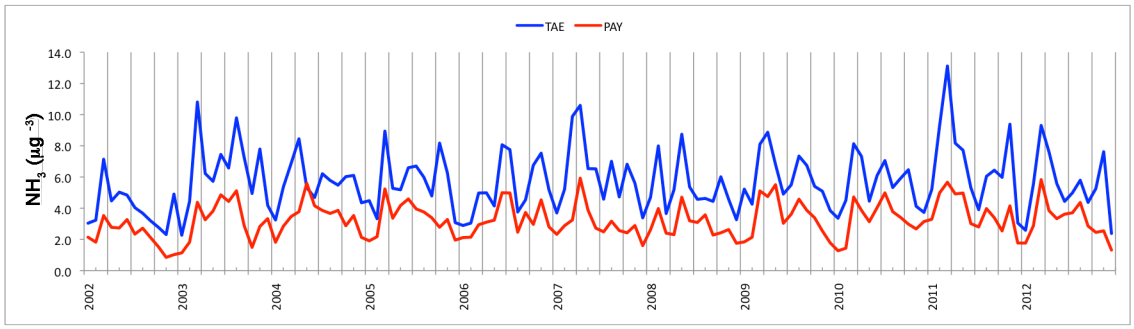

Figure 3: Monthly variation of measured ammonia concentrations at Taenikon (blue) and Payerne (red) between 2002 and 2012 (data provided by FUB).

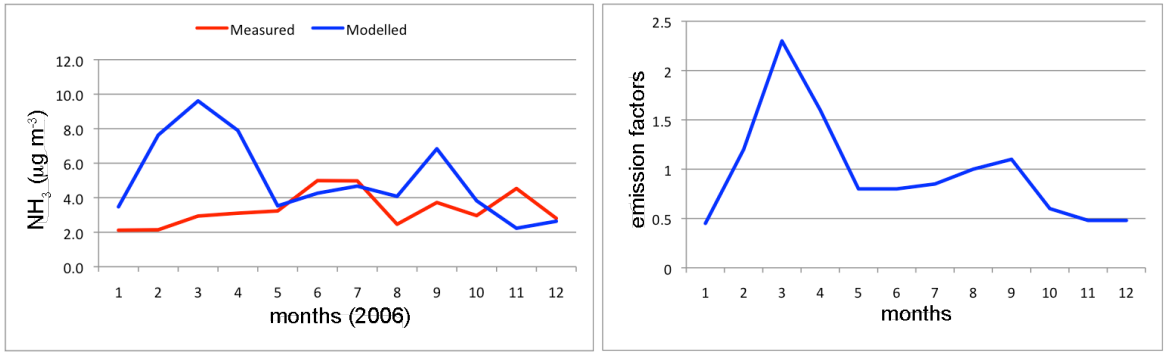

Figure 4: Monthly variation of modeled (blue) and measured (red) (from FUB) NH_3 concentrations at Payerne in 2006 (left) and the time profile of emission factors for NH_3 from agriculture given by the European TNO- MACC emission inventory (right).

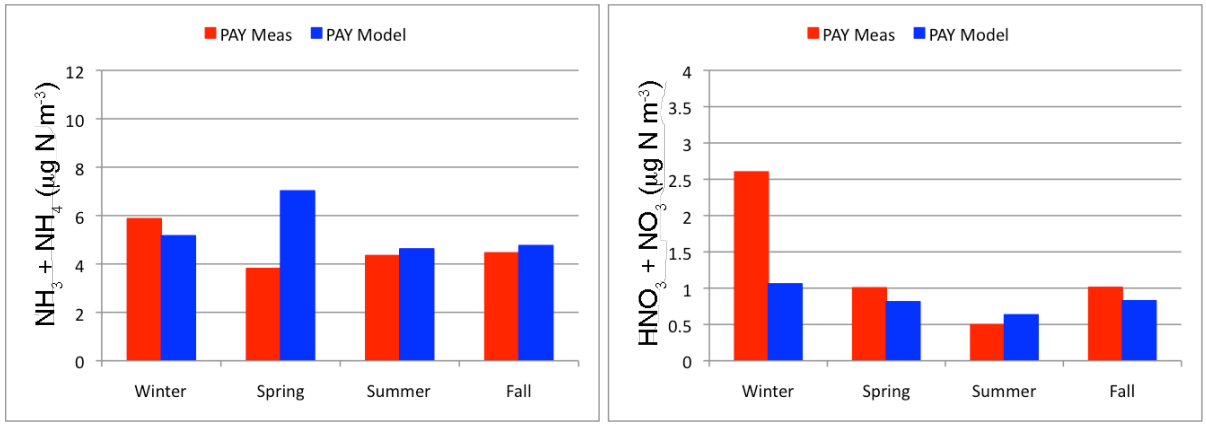

Figure 5: Seasonal variation of measured (red) and modeled (blue) total ammonia (left) and total nitrate (right) at Payerne (NABEL Station) (2006).

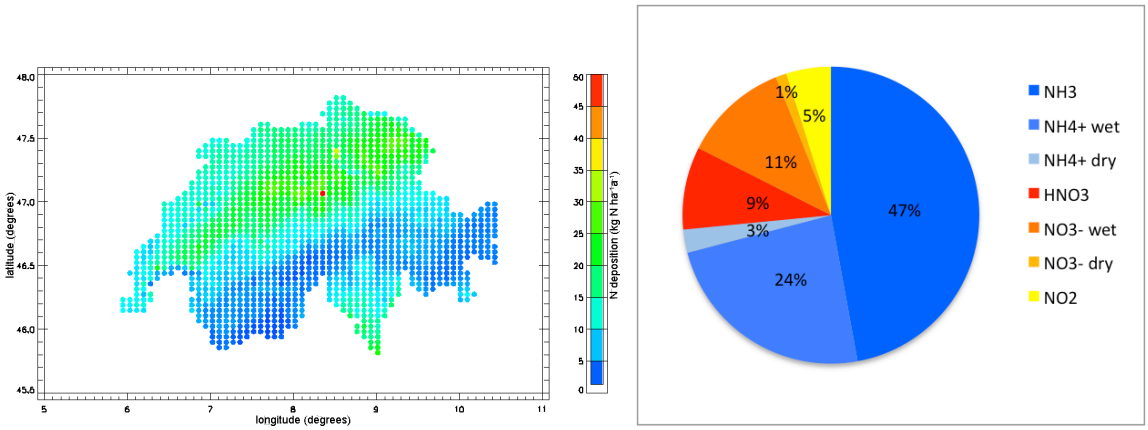

Figure 6: Modeled N deposition in 2006 (kg N ha^{-1} y^{-1}) in Switzerland (left) and relative contribution of oxidized (red, orange, yellow) and reduced (blue tones) components to dry (65%) and wet (35%) deposition (right).

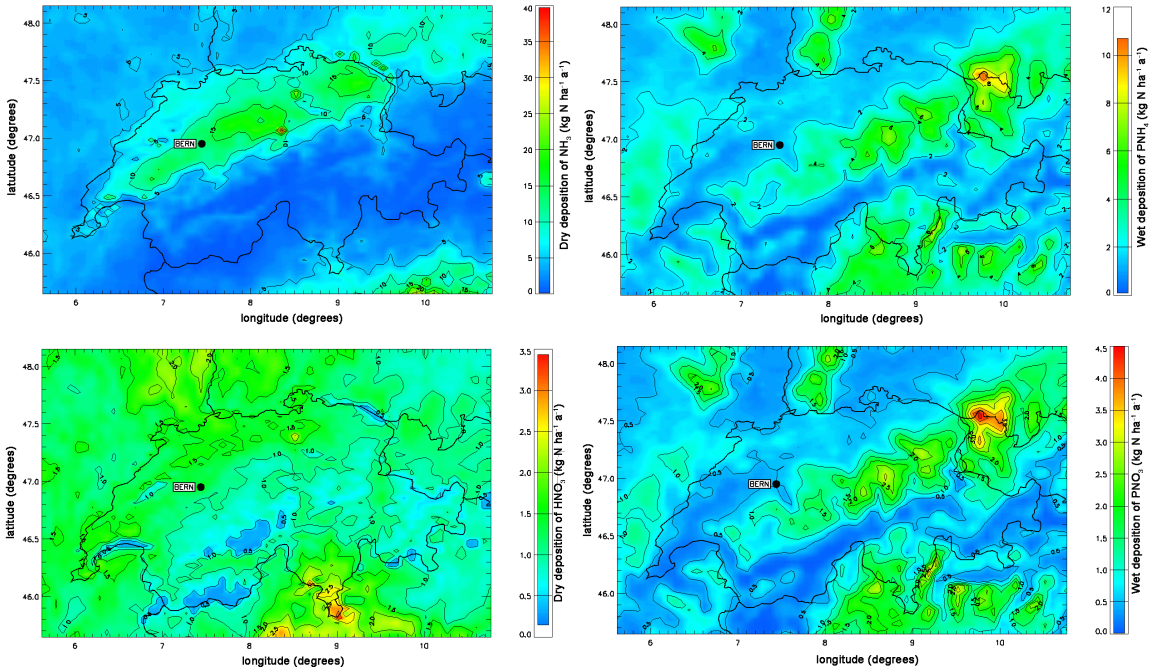

Figure 7: Modeled dry deposition of NH_3 (left upper panel), wet deposition of particulate NH_4^+ (right upper panel), dry deposition of HNO_3 (left lower panel) and wet deposition of particulate NO_3^- (right lower panel) in 2006 (kg N ha^{-1} y^{-1}).

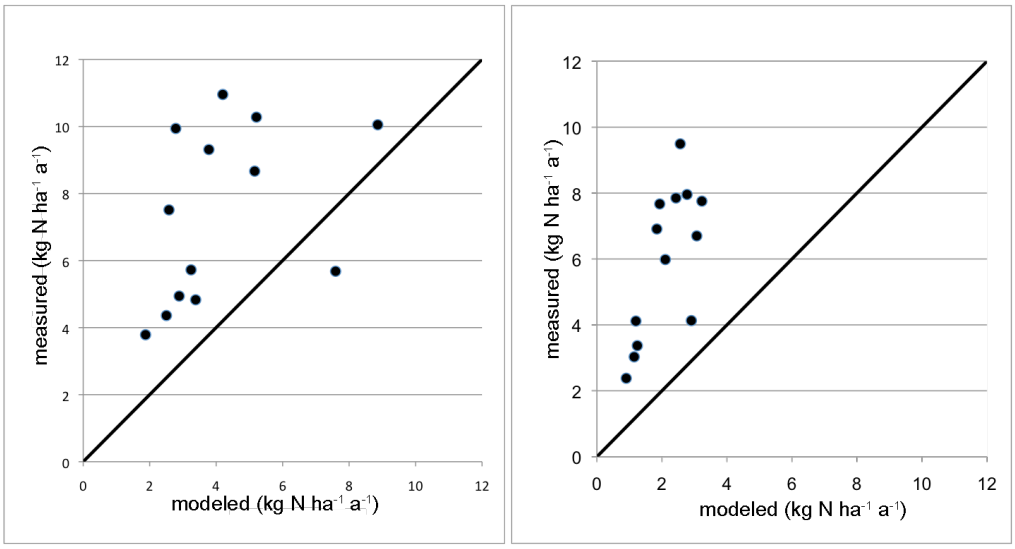

Figure 8: Measured versus modeled wet NH_4^+ (left) and NO_3^- (right) deposition at 13 sites in Switzerland in 2006. Measurements were provided by the Swiss Federal Office of Environment (FOEN)

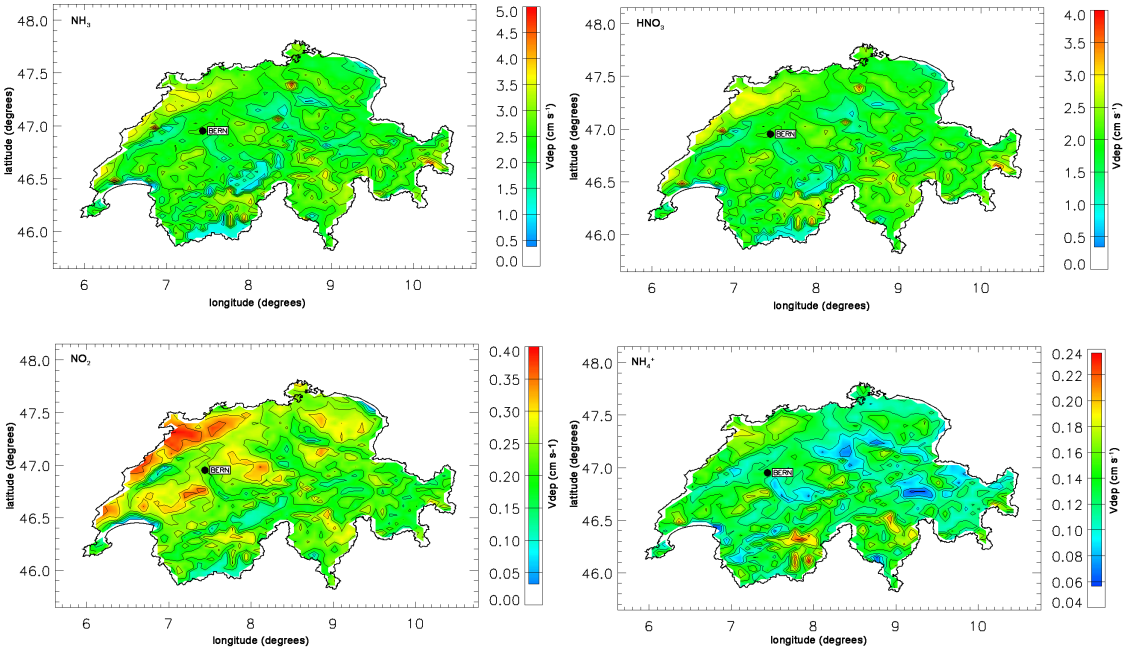

Figure 9: Spatial distribution of annual average dry deposition velocities (cm s^{-1}), upper panels: NH_3 (left), HNO_3 (right), lower panels: NO_2 (left) and NH_4^+ (right).

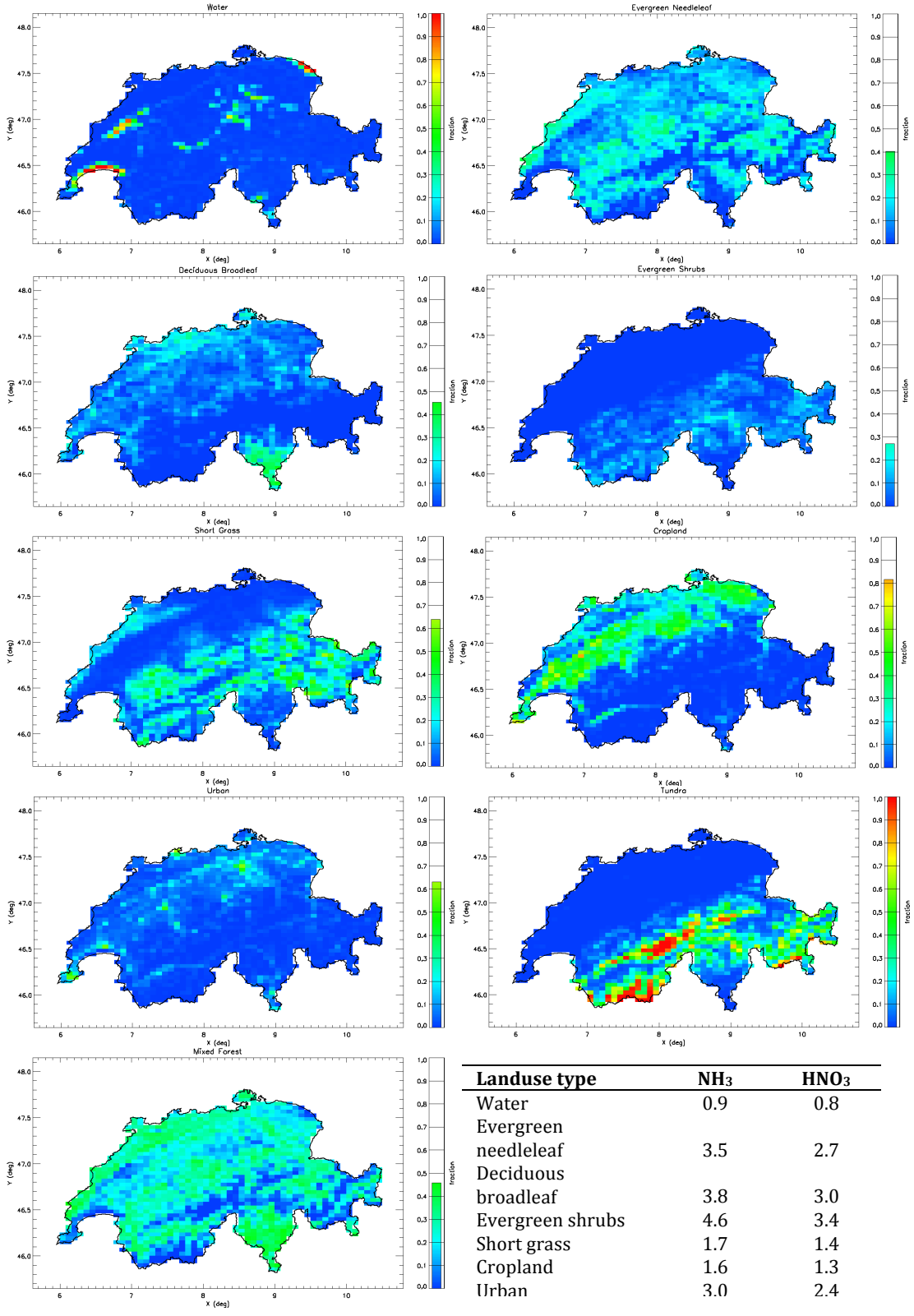

Landuse type	NH_3	HNO_3
Water	0.9	0.8
Evergreen needleleaf	3.5	2.7
Deciduous broadleaf	3.8	3.0
Evergreen shrubs	4.6	3.4
Short grass	1.7	1.4
Cropland	1.6	1.3
Urban	3.0	2.4

Figure 10: Fractional distribution of land-use types in grid cells of the Swiss domain and annual average dry deposition velocities (cm s^{-1}) of NH_3 and HNO_3 on these land-use types (Table).

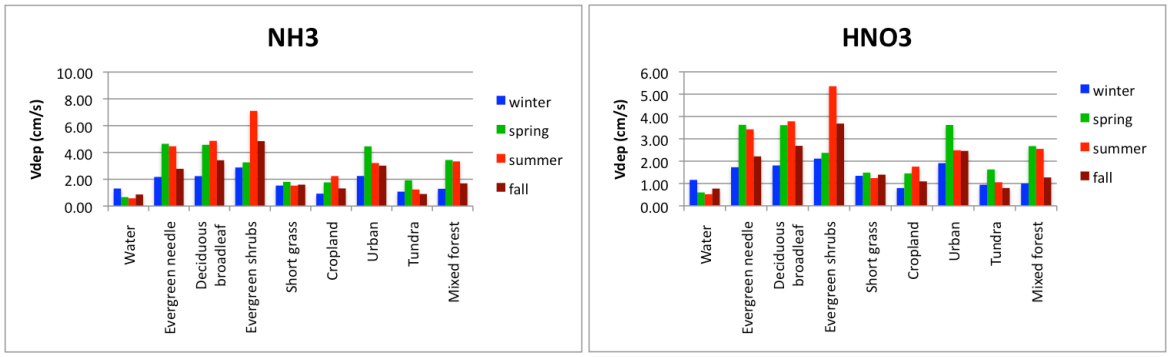

Figure 11: Seasonal variation of dry deposition velocity (cm s^{-1}) for NH_3 (left) and HNO_3 (right) in 2006.